

Soft Sphere Packings at Finite Pressure but Unstable to Shear

Simon Dagois-Bohy,^{1,2} Brian P. Tighe,^{2,3} Johannes Simon,¹ Silke Henkes,^{2,4} and Martin van Hecke¹

¹Kamerling Onnes Lab, Universiteit Leiden, Postbus 9504, 2300 RA Leiden, The Netherlands

²Instituut-Lorentz, Universiteit Leiden, Postbus 9506, 2300 RA Leiden, The Netherlands

³Delft University of Technology, Process & Energy Laboratory,
Leeghwaterstraat 44 2628 CA Delft, The Netherlands

⁴Physics Department, Syracuse University, Syracuse, NY 13244, USA

(Dated: October 9, 2018)

When are athermal soft sphere packings jammed? Any experimentally relevant definition must at the very least require a jammed packing to resist shear. We demonstrate that widely used (numerical) protocols in which particles are compressed together, can and do produce packings which are unstable to shear — and that the probability of generating such packings reaches one near jamming. We introduce a new protocol that, by allowing the system to explore different box shapes as it equilibrates, generates truly jammed packings with strictly positive shear moduli G . For these packings, the scaling of the average of G is consistent with earlier results, while the probability distribution $P(G)$ exhibits novel and rich scalings.

PACS numbers: 05.70.Jk, 05.10.-a, 62.20.D-

Foams, emulsions, colloidal suspensions, granular media and other particulate media undergo a jamming transition when their constituent particles are packed densely enough [1–7]. This transition has been extensively studied in packings of deformable, athermal, frictionless spheres interacting through purely repulsive contact forces [8–12]. The limit where the particles just touch then plays the role of an unusual critical point, as a host of quantities, such as shear modulus, time and length scales, and contact number exhibit power law scaling with the distance to this critical point [8–17].

Numerically created particle packings play a central role in many fields of physics, in particular jamming. In all numerical jamming studies we are aware of, packings are created by compressing a collection of particles, either by inflating the particles or shrinking the simulation box [8–17]. It is then widely believed and tacitly assumed that, when compressed, the system simultaneously develops a finite pressure, a finite yield threshold [9, 10] and a positive shear modulus G [8–13]. Here we demonstrate that, to the contrary, algorithms that work solely by compression tend to produce packings that are unstable to shear, and hence have negative shear moduli. Nevertheless, such ‘improperly jammed’ packings possess a positive pressure P and a positive bulk modulus, and are in mechanical equilibrium — see Fig. 1a.

In this Letter, we probe and explain this anomaly. The root problem is that compression only (CO) algorithms ignore the global shear degrees of freedom. We find that this results in a fraction of improperly jammed CO packings which reaches *one* at the critical point. Hence, compression alone does not lead to jammed packings, and previous results on jamming have considered packings that, instead of being jammed, have been linearly unstable to shear — in particular near jamming.

Furthermore, we remedy this anomaly by introducing

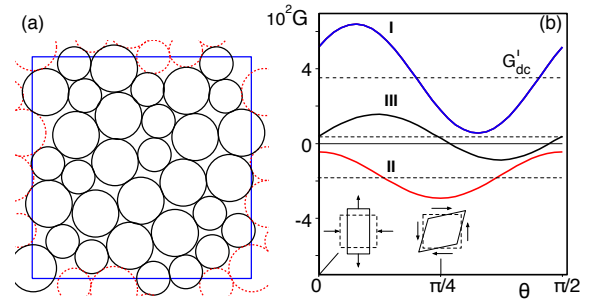


FIG. 1: (Color online) (a) Example of a well-equilibrated CO packing of $N = 32$ particles which is unstable to shear (pressure $P = 10^{-2}$, bulk modulus $K \approx 0.385$, contact number $z \approx 4.26$). (b) Illustration of the sinusoidal angular dependence of G on the principle direction of shear, θ , for three different packings at the same N and P — curve III corresponds to the packing shown in (a), and dashed lines indicate G_{DC} , the angular average of G .

a shear stabilized (SS) packing algorithm that produces truly jammed packings with positive definite shear moduli [18], and probe the probability distribution of G , uncovering novel scaling with distance to jamming and system size.

Shear moduli in CO Packings — We have generated 2D packings of N soft harmonic bidisperse disks (with unit spring constant [11]) by a standard CO packing generating algorithm, for pressures P ranging from 10^{-6} to 10^{-1} and $16 \leq N \leq 1024$. Prior studies of the shear modulus have focused on ensemble averages at fixed distance to the jamming point (P), typically for large N , and without reference to the angular dependence of G .

As illustrated in Fig. 1b, fluctuations and anisotropy are key: G varies sinusoidally with θ , and its angular average, G_{DC} , varies substantially with realization. We

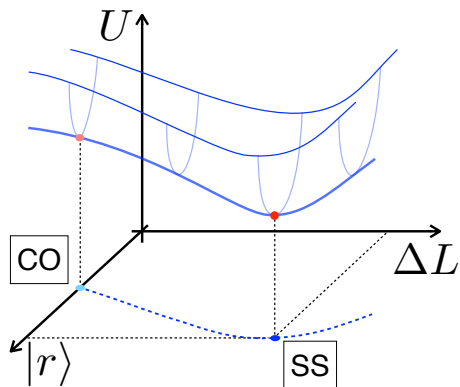


FIG. 2: (Color online) Energy landscape where $|r\rangle$ denotes the particle degrees of freedom, and ΔL the box-shape. CO packings sit at a minimum of U with respect to $|r\rangle$; SS packings sit at a minimum with respect to both $|r\rangle$ and ΔL .

distinguish three types of packings. (I) Truly jammed packings for which $G(\theta) > 0$. (II) Improperly jammed packings for which $G(\theta) < 0$ (III) Improperly jammed packings for which $G(\theta)$ becomes negative over an interval in θ . We stress that all these packings are in a mechanical equilibrium and have a positive bulk modulus.

It has been customary to measure G along a fixed direction [10, 15, 20–24], and the limited unstable range of type III packings, combined with the rare occurrence of type II packings, may explain why these instabilities have escaped attention to date. Since simulations often produce some “problematic” packings (for example due to issues with convergence), packings of types II and III have likely been treated as “bad apples” and thrown out of the ensemble [25, 26].

Boundaries and Shear Stabilization — Improperly jammed packings are not caused by numerical artifacts but stem from the essence of compression only (CO) algorithms. Consider the potential energy landscape as a function of the particle positions, $|r\rangle$, and shear deformations of the box, $|\Delta L\rangle$ (Fig. 2). CO algorithms fix the unit cell and generate packings at a minimum of U with respect to $|r\rangle$. Residual shear stresses and shear moduli correspond to the first and second derivatives, respectively, of U along a strain direction ΔL — without permitting the strain degrees of freedom to equilibrate, both the residual stress and shear modulus are uncontrolled.

To create packings that are guaranteed to be stable against shear in all directions, we include shear deformations of the box and search for local energy minima of U (Fig. 2) [27]. We combine standard conjugate gradient techniques [26] with the FIRE algorithm [28], which improves the speed by an order of magnitude, and also precisely control the pressure of the resulting packings. Since the energy is at a minimum with respect to the

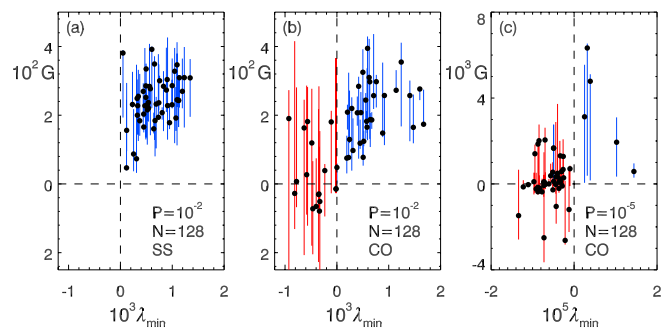


FIG. 3: (Color online) Scatter plots of λ_{\min} vs G for 50 packings of $N = 128$ and P as indicated. Dots correspond to $G(\theta = 0)$, and blue (red) lines indicate the range of $G(\theta)$ when the minimum of $G(\theta)$ is positive (negative). The right bottom quadrant is empty: when $\lambda_{\min} > 0$, G is positive definite. (a) SS packings. (b) CO packings at $P = 10^{-2}$. (c) CO packings at $P = 10^{-5}$ — close to jamming, the fraction of improperly jammed CO packings grows dramatically.

shear degrees of freedom, these packings have strictly positive values of G and exhibit zero residual shear stress [27], unlike CO states. However, as a result of equilibrating the strain degrees of freedom, the unit cell is no longer square. For example, starting from a CO packing (minimum of U with respect to $|r\rangle$), the box is deformed to find a minimum in the extended space spanned by $|r\rangle$ and the strain coordinates (Fig. 2). Such deformations are small for large systems [29].

A formal way of capturing the role of the boundaries is in terms of the stiffness matrices \hat{K}^0 and \hat{K} , where \hat{K}^0 is the usual Hessian, while the “extended Hessian” \hat{K} , introduced in a different context in Ref. [17], includes the dependence on the shear degrees of freedom — for details see the supplementary material. It can then be shown that $G(\theta)$ is positive definite for all θ if all eigenvalues of \hat{K} are *positive* (excluding the trivial zero energy translational modes). Defining λ_{\min} as the minimal eigenvalue of \hat{K} , the sufficient condition for a packing to be stable against shear is $\lambda_{\min} > 0$. In contrast, a positive spectrum for the usual Hessian \hat{K}^0 only guarantees stability in a box with fixed boundaries, but does not guarantee stability to all possible shear deformations (Fig. 1 and 2), contrary to the claim in Ref. [30].

Scatter plots of shear modulus and λ_{\min} for CO and SS ensembles shown in Fig. 3 confirm our picture: (i) All SS packings have positive λ_{\min} and G . (ii) CO packings can have negative λ_{\min} . Although many of these $\lambda_{\min} < 0$ packings are stable when sheared along a fixed direction (dots correspond to $\theta = 0$), they almost always have negative G when sheared along other directions.

Fraction of improperly jammed CO packings — What fraction of CO packings is unstable to shear? What governs the scaling of this fraction? Fig. 4 shows that the probability that CO packings have shear directions along which G is negative, $P_{G<0}$, reaches one near jamming,

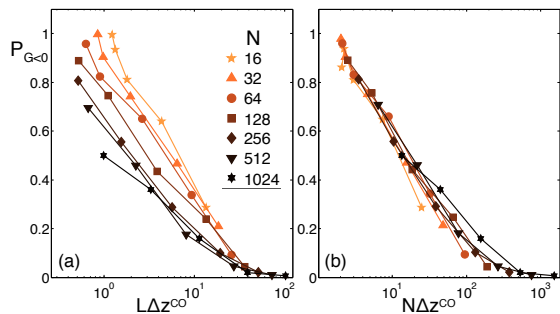


FIG. 4: (Color online) The fraction of CO packings unstable to shear collapses when plotted as function of the excess number of contacts, $N\Delta z^{\text{CO}}$, where $\Delta z^{\text{CO}} := z - z_{\text{iso}}^{\text{CO}} = z - 4 + 4/N$.

and that larger packings need lower pressures for these instabilities to become dominant. It is natural to expect that $P_{G<0}$ would collapse when plotted as a function of L/l^* , where l^* is a characteristic length-scale which diverges as $1/\Delta z$ near jamming, and where Δz is the difference between the contact number z and its value at the jamming point [11, 12, 15, 31–33]. Surprisingly, Fig. 4 shows that the number of excess contacts $\sim N\Delta z$, not the characteristic length scale l^* , governs the fraction of improperly jammed packings — note that we have included a finite size correction to Δz (see below).

We conclude that the standard view of the jamming transition, in which rigidity is attained by simply compressing particles together [10–12], needs a revision: when the pressure is lowered in *finite* CO packings, more and more packings will become unstable to shear, leading to a blurring of the (un)jamming transition. We stress that many excess contacts are needed to avoid improperly jammed CO packings: for example, one needs of the order of a hundred excess contacts for $P_{G<0} < 0.1$.

Scaling of Contact Number and G — Do the same scaling laws for, e.g., z or G [11, 12], govern both CO and SS packings? To answer this question, we have performed a finite size scaling analysis of both SS and CO packings: both the distance to jamming and the system size play a crucial role [34].

We first consider the contact number z [9–12, 35]. A packing is called isostatic when the number of constraints, C , equals $N_{\text{dof}} - N_0$, the number of degrees of freedom N_{dof} minus the number of rigid body modes N_0 . There is one constraint for each of the $N_c \equiv Nz/2$ force bearing contacts [36]. In two dimensions, $N_0 = 2$, corresponding to two rigid body translations (rotation is incompatible with periodic boundary conditions). Hence:

$$z_{\text{iso}} \geq \frac{2}{N}(N_{\text{dof}} - N_0). \quad (1)$$

For CO states in two dimensions, $N_{\text{dof}} = 2N$ (the particle displacements), so that $z_{\text{iso}}^{\text{CO}} = 4 - 4/N$. For SS states

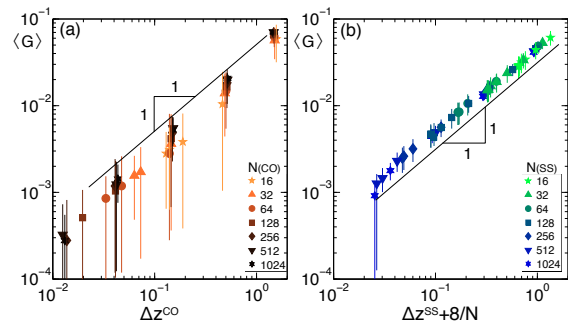


FIG. 5: (Color online) (a) Linear scaling of $\langle G \rangle$ with Δz^{CO} for CO packings. The errorbars indicate the RMS fluctuations in G . (b) Linear scaling of $\langle G \rangle$ with $\Delta z^{\text{SS}} + 8/N$ for SS packings — where $\Delta z^{\text{SS}} := z - z_{\text{iso}}^{\text{SS}} = z - 4$.

the particle displacements are augmented by two shear degrees of freedom, leading to $z_{\text{iso}}^{\text{SS}} = 4$.

Is the isostatic bound reached at unjamming? We have found that both CO and SS packings have one contact in excess of their respective isostatic values when approaching the jamming point (see Suppl. Mat.). Goodrich *et al.* have argued that this extra contact reflects the requirement that jammed states have positive bulk modulus, which puts an additional constraint on the box size [37].

We now turn our attention to the scaling of G , and first investigate the scaling of the angle-averaged shear modulus $\langle G \rangle$ in ensembles of finite sized CO and SS packings. In Fig. 5a we show that in the CO ensemble, $\langle G \rangle$ is proportional to $z - z_{\text{iso}}^{\text{CO}}$, consistent with prior results [10, 15, 17, 24, 37]. In Fig. 5b we show that in the SS ensemble, the average shear modulus is proportional to $z - (z_{\text{iso}}^{\text{SS}} - 8/N)$. So, although the SS shear modulus is also linear in z , its vanishing point extrapolates to a state with four contacts less than the isostatic state. We note that in both ensembles $\langle G \rangle$ is of order $1/N$ in the zero pressure limit.

The amount of scatter in $\langle G \rangle$ observed in our new CO packings is surprisingly large. We note that previous work did not consider the value of G over all angles and discarded negative values of G , which leads to a smaller scatter [25, 26]. Recent work by Goodrich *et al.* shows that this scatter can be further suppressed by using exceptionally accurate equilibration and larger ensembles [37]. Nevertheless, the observation that SS data exhibits far lower scatter than CO data, while both packings were obtained with the same numerical accuracy, suggests that remnants of the unstable modes present in the CO ensemble hinder accurate equilibration.

With few exceptions [10, 15, 16, 38–42], studies of jamming have focused on ensemble averages. Here we consider the probability distribution $P(G)$ for both ensembles, sampling both θ and realizations. Fig. 6a illustrates that for CO packings, $P(G)$ often peaks at *negative* G ,

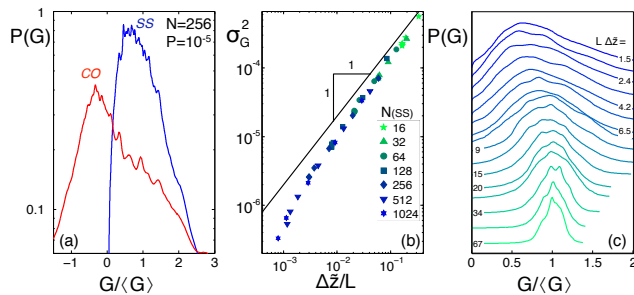


FIG. 6: (Color online) (a) The probability distributions for G of CO and SS packings differ qualitatively. (b) Scaling of the variance $\langle(G - \langle G \rangle)^2\rangle$ for SS packings reveals novel scaling. (c) $P(G/\langle G \rangle)$ shows a systematic variation with $L\Delta \tilde{z}$.

and can possess an extended tail towards negative G . In contrast, for SS packings, G is strictly positive, and the peak of $P(G)$ is always at finite G .

For SS packings, the distributions $P(G)$ are well-behaved; however, there is no single parameter scaling. For brevity of notation, we define $\tilde{z} \equiv 4 - 8/N$, so that $\langle G \rangle \sim z - \tilde{z} \equiv \Delta \tilde{z}$. Our data shows that the variance σ_G^2 scales roughly linear with $\Delta \tilde{z}/L$ (Fig. 6b). The scalings of the average and variance of G suggest that distributions of $P(G/\langle G \rangle)$ that have equal values of $L\Delta \tilde{z}$ might collapse. Fig. 6c shows that grouping $P(G/\langle G \rangle)$ by $L\Delta \tilde{z}$ captures the main trends: for large $L\Delta \tilde{z}$, the distribution $P(G/\langle G \rangle)$ is clearly peaked away from zero, but for lower values of $L\Delta \tilde{z}$ becomes more skewed and wider. We note that the scaling of $P(G < 0)$ for CO packings suggest that finite size scaling corrections for $P(G)$ differ between CO and SS packings, and an important question for the future is to probe these differences [43].

Discussion — Improperly jammed CO packings dominate in the critical, near jamming regime, whereas packings made by a shear stabilized algorithm are strictly jammed: boundary conditions play a crucial role in controlling the rigidity of packings, in particular close to jamming. In most experimental procedures, the creation history is richer than homogeneously inflating particles, and involves the motion of boundaries and shear [1, 3–7, 44] — how does this relate to our scenario? First, we note that in contrast to the ‘shear jammed packing’ of Bi *et al.* [44], our CO and SS packings only exhibit small contact anisotropies that vanish as $1/\sqrt{N}$ [34], and that CO packings exhibit similarly weak anisotropies in the contact forces — we use shear to stabilize, rather than jam. Second, we note that the strong anisotropy of G that we observe is reminiscent of fragility as introduced by Cates *et al.*, although usually fragile states are defined as having no resistance to shear in certain directions (i.e., $G = 0$), while here we have $G < 0$. Moreover, such fragility typically arises due to the shear history of the system [44, 45]. Nevertheless, it is conceivable that protocols that do not explicitly perform shear stabiliza-

tion initially yield improperly jammed states, which then relax until they reach a fragile state.

We acknowledge discussions with C. Goodrich, A. Liu, S. Nagel and Z. Zeravic. SD-B acknowledges funding from the Dutch physics foundation FOM and BPT from the Netherlands Organization for Scientific Research.

- [1] T. S. Majmudar, M. Sperl, S. Luding, and R. P. Behringer, *Phys. Rev. Lett.* **98**, 058001 (2007).
- [2] F. Lechenault, O. Dauchot, G. Biroli, and J. P. Bouchaud, *EPL* **83**, 46003 (2008).
- [3] M. Jerkins, M. Schröter, H. L. Swinney, T. J. Senden, M. Saadatfar, and T. Aste, *Phys. Rev. Lett.* **101**, 018301 (2008).
- [4] M. Clusel, E. I. Corwin, A. O. N. Siemens, and J. Brujic, *Nature* **460**, 611 (2009).
- [5] G. Katgert and M. van Hecke, *EPL* **92**, 34002 (2010).
- [6] X. Cheng, *Phys. Rev. E* **81**, 031301 (2010).
- [7] J.-F. Métayer, D. J. S. III, C. Radin, H. L. Swinney, and M. Schröter, *EPL (Europhysics Letters)* **93**, 64003 (2011).
- [8] F. Bolton and D. Weaire, *Phys. Rev. Lett.* **65**, 3449 (1990).
- [9] D. J. Durian, *Phys. Rev. Lett.* **75**, 4780 (1995).
- [10] C. S. O’Hern, L. E. Silbert, A. J. Liu, and S. R. Nagel, *Phys. Rev. E* **68**, 011306 (2003).
- [11] M. van Hecke, *J. Phys. Cond. Matt.* **22**, 033101 (2010).
- [12] A. J. Liu and S. R. Nagel, *Annual Review of Condensed Matter Physics* **1**, 347 (2010).
- [13] H. P. Zhang and H. A. Makse, *Phys. Rev. E* **72**, 011301 (2005).
- [14] L. E. Silbert, A. J. Liu, and S. R. Nagel, *Phys. Rev. Lett.* **95**, 098301 (2005).
- [15] W. G. Ellenbroek, E. Somfai, M. van Hecke, and W. van Saarloos, *Phys. Rev. Lett.* **97**, 258001 (2006).
- [16] B. P. Tighe and T. J. H. Vlugt, *Journal of Statistical Mechanics: Theory and Experiment* p. P04002 (2011).
- [17] B. P. Tighe, *Phys. Rev. Lett.* **107**, 158303 (2011).
- [18] The distinction between CO and SS packings is comparable to the difference between what Torquato *et al.* refer to as collectively and strictly jammed packings, although these concepts are defined for hard particles [19].
- [19] S. Torquato and F. Stillinger, *J. Phys. Chem B* **105**, 11849 (2001).
- [20] C. S. O’Hern, S. A. Langer, A. J. Liu, and S. R. Nagel, *Phys. Rev. Lett.* **88**, 075507 (2002).
- [21] C. E. Maloney and A. Lemaître, *Phys. Rev. E* **74**, 016118 (2006).
- [22] E. Somfai, M. van Hecke, W. G. Ellenbroek, K. Shundyak, and W. van Saarloos, *Phys. Rev. E* **75**, 020301(R) (2007).
- [23] M. Wyart, H. Liang, A. Kabla, and L. Mahadevan, *Phys. Rev. Lett.* **101**, 215501 (2008).
- [24] A. Zaccane and E. Scossa-Romano, *Phys. Rev. B* **83**, 184205 (2011).
- [25] W. G. Ellenbroek, C. S. O’Hern (private communication).
- [26] C. Schreck and C. O’Hern, *Computational methods to study jammed systems* (Cambridge University Press, 2010).

- [27] To obtain positive G , in principle one only requires the sign of the curvature of U , $\partial^2 U / \partial \gamma^2$, to be positive. At a minimum of U , $\partial U / \partial \gamma = 0$ as well, leading to states with zero residual shear stress.
- [28] E. Bitzek, P. Koskinen, F. Gähler, M. Moseler, and P. Gumbsch, Phys. Rev. Lett. **97**, 170201 (2006).
- [29] We stress here that these anisotropies pertain to individual packings — ensembles of CO or SS packings are isotropic.
- [30] C. S. O’Hern, L. E. Silbert, A. J. Liu, and S. R. Nagel, Phys. Rev. E **70**, 043302 (2004).
- [31] For harmonic particles, $\Delta z \sim P^{1/2}$ [11, 12]
- [32] A. V. Tkachenko and T. A. Witten, Phys. Rev. E **60**, 687 (1999).
- [33] M. Wyart, S. R. Nagel, and T. A. Witten, EPL **72**, 486 (2005).
- [34] S. Dagois-Bohy, B. P. Tighe and M. van Hecke, in preparation
- [35] S. Alexander, Phys. Rep **296**, 65 (1998).
- [36] Here N denotes the number of particles after a small fraction of non-force bearing particles, or “rattlers,” have been removed.
- [37] C. Goodrich, S. R. Nagel and A. J. Liu, arXiv:1204.4915.
- [38] S. Henkes, C. S. O’Hern, and B. Chakraborty, Phys. Rev. Lett. **99**, 038002 (2007).
- [39] B. P. Tighe, A. R. T. van Eerd, and T. J. H. Vlugt, Phys. Rev. Lett. **100**, 238001 (2008).
- [40] W. G. Ellenbroek, M. van Hecke, and W. van Saarloos, Phys. Rev. E **80**, 061307 (2009).
- [41] C. Heussinger, P. Chaudhuri, and J.-L. Barrat, Soft Matter **6** (2010).
- [42] B. P. Tighe, E. Woldhuis, J. J. C. Remmers, W. van Saarloos, and M. van Hecke, Phys. Rev. Lett. **105**, 088303 (2010).
- [43] C. Goodrich, A. J. Liu, S. R. Nagel, Priv. Comm.
- [44] D. Bi, J. Zhang, B. Chakraborty, and R. P. Behringer, Nature **480**, 355 (2011).
- [45] M. E. Cates, J. P. Wittmer, J.-P. Bouchaud, and P. Claudin, Phys. Rev. Lett. **81**, 1841 (1998).

Supp Material

Extended Hessian — A packing’s linear response to shear can be expressed as a matrix equation. Let us introduce $|u\rangle = |\{u_i^x, u_i^y\}_{i=1}^N\rangle$, $|q\rangle = |\{u_i^x, u_i^y\}_{i=1}^N, \gamma, \theta\rangle$ and

$$K_{mn}^0 = \frac{\partial^2 U}{\partial u_m \partial u_n} \quad \text{and} \quad K_{mn} = \frac{\partial^2 U}{\partial q_m \partial q_n}, \quad (2)$$

evaluated at the coordinates corresponding to a packing. \hat{K}^0 is the usual Hessian or stiffness matrix, while the “extended Hessian” \hat{K} , introduced in Ref. [17], includes the dependence on γ and θ . The response to imposed strain is the solution to $\hat{K}^0|u\rangle = |F_\Gamma\rangle$ is

an apparent force felt by particles involved in boundary-crossing contacts when the lattice vectors are distorted. It comprises the first $2N$ components of $\hat{K}|\Gamma\rangle$, where $|\Gamma\rangle = |\{0\}_{2N}, \gamma, \theta\rangle$. The quadratic term in the change in potential energy, which governs linear stability, is then $\Delta U/V = (1/2V)\langle q|\hat{K}|q\rangle \equiv (1/2)G(\theta)\gamma^2$, where V is the volume, so that

$$G(\theta) = \langle q|\hat{K}|q\rangle/\gamma^2 V. \quad (3)$$

From Eq. (3) it immediately follows that $G(\theta)$ is positive definite for all θ if all eigenvalues of \hat{K} are *positive* (excluding the trivial zero energy translational modes).

We finally note that Eq. (3) requires the extended Hessian \hat{K} , which includes shear degrees of freedom [17]. To relate G to the usual Hessian \hat{K}^0 , we follow Ref. [21] and write $G\gamma^2/2V = W_a - W_{na}$, where $W_a > 0$ is the work done in affinely displacing the particles and the box. The actual particle displacements $|u\rangle$ have a non-affine contribution $|u_{na}\rangle = |u\rangle - |u_a\rangle$ that reduces the deformation energy by $W_{na} = \langle u_{na}|K^0|u_{na}\rangle/2$. $W_{na} > 0$ if the spectrum of K^0 is non-negative, but G can still be negative if $W_{na} > W_a$. — hence there is no simple relation between the sign of G and the eigenvalues of the usual Hessian \hat{K}^0 .

Contact Numbers for $P \rightarrow 0$ — Based on our counting, the isostatic number of contacts, C_{iso} , equals $2N - 2$ for the CO ensemble, and precisely $2N$ for the SS ensemble. In Fig. 7 we show our results for the excess contact numbers C^+ , defined as the difference between the actual number of contacts C and the respective isostatic value C_{iso} . For both the CO and SS ensembles, the number of excess contacts reaches one in the limit of vanishing pressure: so for 2D CO ensembles, the number of contacts reaches $2N - 1$, and for 2D SS ensembles, the number of contacts reaches $2N + 1$.

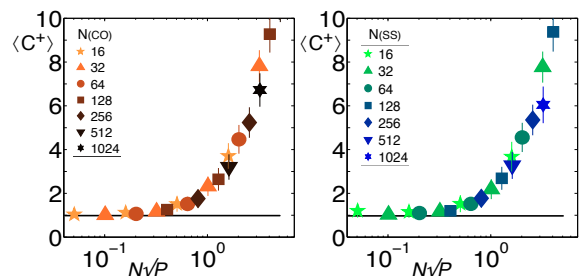


FIG. 7: (Color online) Scaling of the excess contact number of contacts, $C^+ = C - C_{iso}$ for (a) the CO and (b) the SS ensemble.